AD-A040 909   BALLISTIC RESEARCH LABS ABERDEEN PROVING GROUND MD   F/G 20/4
PRESSURE MEASUREMENTS ON A SPINNING WIND TUNNEL MODEL BY MEANS --ETC(U)
MAY 77   A MARK

UNCLASSIFIED   BRL-MR-2750   NL

| OF |
AD
A040 909

END

DATE
FILMED
7-77

BRL MR 2750

AD

BRL

MEMORANDUM REPORT NO. 2750

ADA040909

PRESSURE MEASUREMENTS ON A SPINNING WIND
TUNNEL MODEL BY MEANS OF TELEMETRY

Andrew Mark

DDC
RECEIVED
JUN 24 1977
C

May 1977

USA ARMAMENT RESEARCH AND DEVELOPMENT COMMAND
USA BALLISTIC RESEARCH LABORATORY
ABERDEEN PROVING GROUND, MARYLAND

AD NU.
DDC FILE COPY.

REPORT DOCUMENTATION PAGE		READ INSTRUCTIONS BEFORE COMPLETING FORM
1. REPORT NUMBER BRL MEMORANDUM REPORT NO. 2750	2. GOVT ACCESSION NO.	3. RECIPIENT'S CATALOG NUMBER
4. TITLE (and Subtitle) PRESSURE MEASUREMENTS ON A SPINNING WIND TUNNEL MODEL BY MEANS OF TELEMETRY		5. TYPE OF REPORT & PERIOD COVERED Final rept.
		6. PERFORMING ORG. REPORT NUMBER
7. AUTHOR(s) Andrew/Mark		8. CONTRACT OR GRANT NUMBER(s)
9. PERFORMING ORGANIZATION NAME AND ADDRESS U.S. Army Ballistic Research Laboratory Aberdeen Proving Ground, Maryland 21005		10. PROGRAM ELEMENT, PROJECT, TASK AREA & WORK UNIT NUMBERS RDT&E 1W662618AH80
11. CONTROLLING OFFICE NAME AND ADDRESS US Army Materiel Development & Readiness Command 5001 Eisenhower Avenue Alexandria, Virginia 22333		12. REPORT DATE MAY 1977
		13. NUMBER OF PAGES 31
14. MONITORING AGENCY NAME & ADDRESS(if different from Controlling Office)		15. SECURITY CLASS. (of this report) UNCLASSIFIED
		15a. DECLASSIFICATION/DOWNGRADING SCHEDULE

16. DISTRIBUTION STATEMENT (of this Report)

Approved for public release; distribution unlimited.

BRL-MR-2750

17. DISTRIBUTION STATEMENT (of the abstract entered in Block 20, if different from Report)

18. SUPPLEMENTARY NOTES

19. KEY WORDS (Continue on reverse side if necessary and identify by block number)

Telemetry
Magnus
Pressure Distribution
Wind Tunnel
Transducers

20. ABSTRACT (Continue on reverse side if necessary and identify by block number) (lcb)

The Magnus force is a side force which exists on spin stabilized projectiles at angle of attack. Although its absolute magnitude is small, it has a destabilizing effect and as such is of interest to projectile designers, in the U.S. Army. A large part of the Magnus force arises from an asymmetric pressure distribution caused by the distorted boundary layer. Experimentally, the Magnus effect has always been measured in terms of force by using strain gage balances. This paper discusses a possible technique for measuring the pressure distribution
(Continued)

DD FORM 1473 EDITION OF 1 NOV 65 IS OBSOLETE
1 JAN 73

050 750

20. ABSTRACT (Continued):

about a spinning body and obtaining the force by integration. It would also serve as a check for three dimensional boundary layer calculations presently available. The technique described involves imbedding pressure transducers into the model surface and the use of a miniature, self contained telemetry system to transmit the pressure data out of the tunnel. Data with spin and without spin has been obtained at a single axial location on a tangent-ogive-cylinder. The data without spin compared favorably with theoretical calculation. Data with spin indicated an anomaly in the pressure distribution. There appeared a phase shift of the data in the direction of spin. The system had undergone frequency response testing which appears to be adequate. The only link not thoroughly investigated is the transmitter-antenna system. This is awaiting further funding and the dilemma is at present still unresolved.

TABLE OF CONTENTS

3

LIST OF ILLUSTRATIONS

I. INTRODUCTION

A. Background

When fired from a gun, spin stabilized projectiles experience a side force known as the Magnus force. This is schematically represented in Figure 1. This force is generated on axisymmetric bodies of revolution because of a combination of spin and angle of attack. It is primarily the result of a distorted boundary layer which creates an asymmetric inviscid pressure distribution about the body. Additionally, an asymmetric cross flow contributes a centripetal pressure of a somewhat smaller magnitude. There also exist surface shear stress components in the axial and circumferential directions which contribute to the side force[1]. The effect of the axial shear stress contribution is very small. The circumferential shear force, however, reaches magnitudes comparable to those produced by the centripetal pressure.

It is important to be able to describe the Magnus force on projectiles because of its destabilizing effect. Although its magnitude is relatively small, between one or two orders of magnitude smaller than the normal force, it acts aft of the center of gravity and is, therefore, of concern to projectile designers. Within the last few years at least one U.S. Army projectile, the M483, had experienced flight instability because of an excessive Magnus force.

Besides this free flight inference of the effect of the Magnus force, other, more controlled tests on projectile shapes have been made over the years by several authors[2-4]. All of these observations were wind tunnel force measurements. There are, however, other ways of characterizing the Magnus force. One can, for example, describe at least part of the Magnus force by measuring the static pressure distribution on a spinning model. The detailed distribution can then

1. W. B. Sturek, "Three-Dimensional Boundary Layer Research as Applied to the Magnus Effect on Spinning Projectiles," BRL Memorandum Report No. 2573, U.S. Army Ballistic Research Laboratories, Aberdeen Proving Ground, Maryland, December 1975. AD B008821L.

2. G. I. T. Nielsen and A. S. Platou, "The Effect of Conical Boattails on the Magnus Characteristics of Projectiles at Subsonic and Transonic Speeds," BRL Report No. 1720, U.S. Army Ballistic Research Laboratories, Aberdeen Proving Ground, Maryland, June 1974. AD 921823L.

3. W. H. Curry, J. F. Reed, and W. C. Ragsdale, "Magnus Data on the Standard 10° Cone Calibration Model," SC-DC 71-3821, Sandia Laboratories, Albuquerque, New Mexico, March 1971.

4. A. S. Platou, "Magnus Characteristics of Finned and Non-Finned Projectiles," AIAA Journal, Vol. 3, No. 1, January 1965.

be integrated to yield not only the pressure contributions of the Magnus force, but also drag, lift, and the normal force. Numerical methods for computing pressure distributions on rotating axisymmetric bodies are also available and measured values could thus check the computations[5,6]. At present, we can only compare the integrated pressure against force measurements. A technique which would measure the pressure distribution on spinning wind tunnel models is, therefore, welcome.

Conventional pressure measuring techniques are not applicable because of the rotating model which can reach spin rates up to 30,000 RPM in wind tunnels to simulate the cross flow parameter, pd/2V, for real projectiles. It is possible to install transducers into the model and bring the data out by means of slip rings, but this method is generally limited to a lesser rotation rate. A novel idea by Miller[7] involved a spinning model and a stationary transducer. This technique relies on a tight seal between stationary and moving parts. At present this technique is limited to a spin rate of about 5,000 RPM but with refinements higher spin rates will be achieved. This paper deals with yet another technique for measuring the pressure distribution on spinning models, namely that of using pressure transducers and a self contained telemetry system in the rotating model.

B. Purpose

The purpose of this work is to develop a telemetry technique which can be employed to measure the pressure distribution on spinning wind tunnel models. The ultimate end result is to compare the measured distributions with computations using the numerical techniques developed by Dwyer[5] and to describe the pressure contribution to the Magnus force on projectile shapes of interest to the Army.

The measurement technique will be described in some detail in subsequent sections together with system calibrations. Static pressure data obtained in the wind tunnel are compared to theoretical calcula-

5. H. A. Dwyer, "Methods for Computing Magnus Effects on Artillery Projectiles," BRL Contract Report No. 329, U.S. Army Ballistic Research Laboratory, Aberdeen Proving Ground, Maryland, January 1977. AD A035330.

6. W. B. Sturek, et al, "Computations of Turbulent Boundary Layer Development Over a Yawed Spinning Body of Revolution With Application to the Magnus Effect," International Symposium on Turbulent Shear Flows, The Pennsylvania State University, University Park, Pennsylvania, 18-20 April 1977. Also to be published as a BRL Report.

7. M. Miller, "A Technique to Measure the Pressure Distribution Acting on the Surface of a Spinning Body in a Wind Tunnel," ED-TR-76070, September 1976.

tions under a no spin condition. Data with spin are then presented and some of the accompanying anomalies discussed.

II. MEASUREMENT TECHNIQUE

The idea for the technique of telemetering pressure out of a wind tunnel comes to the author quite naturally as the result of working in an environment where telemetry methods have been employed in the measurement of temperature and angle of attack on projectiles fired from guns. The techniques of g-hardening the electronic components have been developed over the last ten years at BRL and other places. This normally involves using solid state devices and encapsulating them in an epoxy based resin. It seemed natural to extend this expertise to a wind tunnel model instrumented with pressure transducers and a telemetry system contained within it to test the feasibility of this idea.

A. Wind Tunnel Model

The tests were carried out at the BRL Supersonic Wind Tunnel No. 1 from Mach 2.0 to 3.5 in increments of .5. The boundary layer was artificially tripped with an abrasive band and spark shadowgraph enlargements of the boundary layer indicated turbulent flow.

The model was a 5.715 cm (2.25 inches) diameter, 7.1 caliber tangent-ogive-cylinder with a 3 caliber nose. A cutaway schematic of the model and its internal features is illustrated in Figure 2. The double crosshatched portion remained stationary while the single crosshatched portion rotated. Rotation was provided by air introduced through the sting and channeled through turbine-like vanes at the rear of the model. Spin rates of up to 20,000 RPM were obtained by means of this method. This upper limit of rotation rate was established as a safe maximum after dynamical balancing of the model. This arbitrary maximum was sufficiently high for the purpose of the tests. The model was constructed in several sections as depicted in the figure. Each section was bored out to accommodate portions of the telemetry system. The nose section housed the power for the whole system in the form of rechargeable Ni-Cad batteries plus some signal conditioning components. The center section contained the transducers, amplifiers, and the transmitter. It should be pointed out that the present work has measured pressure at one axial station only (X = 3.14 calibers) to try the technique. There are no reasons why transducers located at many axial stations, of sufficient number to describe the distribution with reasonable smoothness, could not be used with the same system. The transmitting antenna was simply a 1/16 inch copper-clad fiberglass board which was secured to the rotating portion of the model. The stationary receiving antenna lay adjacent to the transmitting antenna and was secured to the sting housing. The signal was carried to a tape recorder by means of a shielded cable from the receiving antenna

9

through the sting. To facilitate the understanding of the transmission link, a block diagram discussion will follow with the aid of Figure 3.

B. Telemetry System

The basic telemetry system employed is an FM/FM system. It consists of two channels of data. Two transducers were used on the model to sense pressure 180° apart. The output of one of the transducers was fed out of the system directly to yield absolute pressure whereas the second was electronically combined with first to yield differential pressure. This was accomplished in the following way. Two transducers, labeled A and B in Figure 3, were amplified to a 5 volt level at the maximum anticipated surface pressure of 5 psia. This high level output was then split, one part driving a 70 kHz subcarrier oscillator 15% and the other part used as the input to a differential amplifier. The output of transducer B was directly fed into the differential amplifier. This amplifier was set at unit gain and the output deviated a 90 kHz subcarrier oscillator 15%. The net result was two channels of data labeled PSIA and PSID in Figure 3. These were mixed and amplified to deviate a 250 MHz transmitter about a 100 kHz. The power of the transmitter was approximately 100 mW but since the transmitting and receiving antenna were in close proximity much less power would have been adequate. In the transmission of data, the signal actually recorded on tape consisted of a multiplexed waveform. Both the PSIA and PSID channels would thus be separately retrieved with a discriminator and the pressure amplitude recovered and played out on oscillograph paper. The dotted line in Figure 3 refers to a before test and after test system calibration which was performed by direct comparison to a CEC strain gage transducer. The CEC transducer was calibrated against a dead weight tester to a combined accuracy, linearity, hysteresis of .25%. This calibration was for a temperature variation between 18°C and 21°C (65 to 75°F). Although our runs at Mach 3.0 and 3.5 resulted in recovery temperatures of 10.0°C (50°F) and 14.5°C (58°F) respectively, it was felt that a feasibility study should waste a minimum amount of time in its yielding of information. Therefore, at these Mach numbers a slightly larger calibration error is accepted.

C. The Transducer

The pressure transducers employed for this study were manufactured by Kulite Corporation and are miniature, solid state semiconductor strain gage sensors having a four-active element bridge circuit[8]. The strain gage is diffused into the silicon and is, thus, an integral part of it. These transducers have a natural frequency of approximately 70 kHz. Physically, they looked like a hexhead screw with a 1.11 cm (7/16 inch) 10-32 threaded bolt length. These transducers were simply

---

8. *Kulite Semiconductor Products, Inc., "Notes on Applications of Integrated Sensor (IS) Pressure Transducer," Application Note KPS AN 11.*

screwed into a drilled and tapped hole provided along the centerline of the model. Pressure was sensed through a .159 cm (1/16 inch) diameter port 2.858 cm (1.125 inches) long with a slight "el" near the centerline. The reason for placing the transducers along the centerline was to eliminate any centrifugal forces on the diaphragm. We could not allow any component to fail mechanically or electronically since repairs in the potted state are almost impossible. In case of failure, whole sections of electronic components have to be machine removed and replaced. As mentioned previously, these transducers were calibrated statically in the model from vacuum to 5 psia. We expected absolute pressures from about .5 psi to 5 psi with differentials of .5 to .2 psi. The transducers proved to be extremely linear well below 1% full scale. Cassanto, et al,[9] found similar results for comparable transducers used on reentry-vehicle pressure measurements. These calibrations, however, do not reflect the true nature of the environment in which we will eventually perform the measurements.

The spin environment of 20,000 RPM reflects a 333 Hz frequency response necessary for the port-transducer system. Cassanto, et al,[9] have made frequency response measurements of a Kulite transducer with a port similar to ours in a shock tube. They allowed normal shocks of different strengths to pass over the port and inferred frequency response from the rise time. These results are summarized in Figure 4. The longest port length they tested was 1.778 cm (.7 inch); however, these data can be extrapolated to our length of 2.858 cm (1.125 inches). This is shown by the dashed lines in the figure. It appears that the higher the pressure difference, the higher the cutoff frequency becomes. For our worst case, that of $\Delta P \approx .5$ psi, the cutoff frequency appears to be approximately 4 kHz, way above that required by us (333 Hz). The other check usually performed on a ported system is for a Helmholtz resonance. The one-end-open formula, $f = a/2L$, where "a" is the sonic velocity and "L" is the port length, yields a fundamental of over 800 Hz; again, larger than the largest we expect to encounter. Armed with this information on frequency response we were confident that the central location of the transducer in the model would not jeopardize our ability to measure surface pressure faithfully under rotation. We, therefore, proceeded with the first series of experiments. These were the static tests (without spin) where pressure was measured at various circumferential positions and angles of attack.

III. TESTS WITHOUT SPIN

In the wind tunnel the model was held at a fixed angle of attack, α, and continually rolled through 270° very slowly. It took several

---

9. J. M. Cassanto, et al, "Use of Miniature Solid State Pressure Transducer for R/V Flight Test Application," ISA ASI 74210, 1974, pp. 33-34.

11

minutes to complete one roll cycle. The angles of attack were 0, +4, +8, and +10 degrees. A negative 4° was also included for redundancy. This proved to duplicate the +4° condition. The windward ray is taken to be zero for the circumferential coordinate as depicted in Figure 1. Figures 5 and 6 show the surface pressure results at no spin for Mach 2 and 3 respectively. Results at the other Mach numbers show similar tendencies and are omitted. The solid lines represent continuous data obtained by means of the Kulite transducers and telemetry with the angle of attack as a parameter. The tenths and hundredths units arise from a sting deflection correction due to the normal force. The numerals, 0, 4, and 10 written in at the various roll angles, are calculations by Sturek using Dwyer's scheme[5]. The agreement between calculation and experiment is very good at the lower angles of attack, 0° and 4.2°. Here the discrepancy is only 3% at most. At $\alpha = 10.62°$, however, the discrepancy is 16% for $M = 2$ and 20% for $M = 3$ at the 90° roll angle position. This large difference is due to the fact that the boundary layer has probably separated. In fact, leeside vortices emerge from the boundary layer at approximately $\alpha = 6°$ for this configuration[10].

IV. TESTS WITH SPIN

After the static tests were completed and satisfactory results obtained by comparing them with computations, we were ready to begin our tests with spin. These tests were carried out in the following way. The model, fixed at angle of attack in the wind tunnel, was spun up to more than 20,000 RPM by means of the vaned air turbine in the rear of the model. The air was then turned off and the model permitted to coast to a near stop with friction as the only despinning torque. This process took three to five minutes and it is assumed that unsteadiness in any one revolution during despin was negligible. Revolutions were counted by implanting a small bar magnet in the rotating brass turbine vanes and a coil in the adjacent stator. Each passage of the magnet over the coil induced a voltage pulse which was recorded on a separate channel on the tape recorder. Individual 1 kHz and 10 kHz reference signals were also recorded so that these together with the magnet pulses yielded rotation rate. The angle between the magnet position and one of the transducers was also measured so that the distribution could be accurately located on the model.

It is interesting to view a typical raw pressure trace to obtain an idea as to the quality of signal we obtained. Such an example is pictured in Figure 7. The two timing signals are observed at either end of the graph with the magnet trace near the top. A scale is superimposed on the pressure trace. This happens to be a $M = 2$ trace at $\alpha = 10.62°$. The RPM are noted on the figure as 14634. On this

---

10. BRL unpublished data.

12

scale, the resolution is a little better than .05 psi and since the calibrated accuracy is approximately .5% or say .015 psi the scale could be expanded to yield more detailed information. The present scale is adequate, however, to familiarize the reader with the type of data obtainable from wind tunnel telemetry instrumentation.

Successive graphs present data at M = 2 and M = 3.5. It should be mentioned at the outset that with a telemetry system a tremendous volume of data can be recorded in a short time which would result in many figures if it were all to be presented. Therefore, selected pieces of data are chosen at the extremes of both Mach number and angle of attack.

The M = 2 results are presented in Figures 8 and 9 for $\alpha = 4.20°$ and 10.62° respectively. $\phi = 0$ is the windward meridian and should see the highest pressure. A number of spin rates are parametrized. There appears, however, a noticeable shift in this peak pressure with increasing RPM. The same sort of trend is repeated for the other runs and the M = 3.5 results are depicted in Figures 10 and 11. These types of data have never been obtained experimentally and, thus, can be checked out computationally. Such large shifts in the pressure distribution are not evident in calculations made by Sturek using Dwyer's scheme with spin[5]. At 20,000 RPM the shift in the pressure data amounts to about 80°, always in the direction of spin. It was thought at first that this phenomenon might be due to the fact that data are obtained at X = 3.14 calibers only and, this location being near the point of tangency of the ogive (X = 3 calibers), caused the anomaly because of the expansion at that location. The calculations do not indicate any such trend and other experiment related causes must be sought. There appears also a slight decrease in amplitude at the windward and leeward rays. It was thought that the centrifugal effect on the air column in the port might account for it. It turns out, however, that this correction is only about 2% at 20,000 RPM and is accounted for in the figures presented.

V. DISCUSSION OF RESULTS

The pressure distribution about a spinning body of revolution at angle of attack should behave as indicated in the top part of Figure 12. Under a no spin condition, the meridional plane is as a plane of symmetry. With spin the pressure contribution to the Magnus force comes from a slight clockwise shift of the leeside bubble. This is primarily a displacement thickness effect. The centripetal pressure term for our measuring location (at 3.14 calibers) is an order of magnitude smaller than the displacement effect contribution. The present results as sketched on the bottom of Figure 12 are not possible since this would result in a normal force to the right for a nose-pitched-up projectile. One could argue that the measurement is performed at a single axial station only, and that other stations

13

would produce a correct integrated effect as the bubble swirls around the body for different axial locations. This is unlikely, however, and can be answered only by multiple axial station measurements.

The curious shifts in the data behave very regularly with rotation rate. This is depicted in Figure 13 where the amount of shift in degrees is presented as a function of RPM. An almost linear variation is observed. To date, no satisfactory explanation is available. At the conclusion of the spin tests it was asserted that because of the passageway to the transducer, the frequency response is inadequate, even though extensive tests by Cassanto, et al,[9] showed the system to be very adequate. Nonetheless, a quick test was designed to check the frequency response of these transducers.*

An asymmetric "T" of copper tubing was formed with one side of the "T" approximately 2.858 cm (1.125 inches) long and designed to hold a Kulite transducer. The other side had an effective zero length of tubing with a Kulite transducer attached. The base leg of the "T" was connected to a vibrating pump with a frequency near 300 Hz. The output of the transducers was viewed on a dual trace oscilloscope. Both signals were superposed on the scope resulting in a single trace. The amplitude and phase matched perfectly which meant that for at least a frequency of 300 Hz or so the 2.858 cm (1.125 inches) passage has no affect on the surface pressure. Similar conclusions were reached when the model transducer port was permitted to rotate past a jet of air. No large shifts were observed.

One can conceive of and construct a number of different tests to measure the true nature of the transducer-port system frequency response. These, it is felt, however, would yield results as those just mentioned. The area not totally explored yet is that of the telemetry transmission links. It has been noted that in past similar rotating model experiments a slight misalignment between transmitting and receiving antenna caused phase shifts in the data. We thought this was resolved, however, by having steps machined into the model to accommodate the fiberboard antennas. It could also be that the radiation pattern from the transmitting antenna is not uniform causing a phase shift. A number of thoughts run through the author's mind on various checks and tests that can be performed on the transmission system. These, however, must await future funding.

---

* *This setup was conceived by Clarence C. Bush of the Launch and Flight Division of BRL.*

REFERENCES

1. W. B. Sturek, "Three-Dimensional Boundary Layer Research as Applied to the Magnus Effect on Spinning Projectiles," BRL Memorandum Report No. 2573, U.S. Army Ballistic Research Laboratories, Aberdeen Proving Ground, Maryland, December 1975. AD B008821L.

2. G. I. T. Nielsen and A. S. Platou, "The Effect of Conical Boattails on the Magnus Characteristics of Projectiles at Subsonic and Transonic Speeds," BRL Report No. 1720, U.S. Army Ballistic Research Laboratories, Aberdeen Proving Ground, Maryland, June 1974. AD 921823L.

3. W. H. Curry, J. F. Reed, and W. C. Ragsdale, "Magnus Data on the Standard 10° Cone Calibration Model," SC-DC 71-3821, Sandia Laboratories, Albuquerque, New Mexico, March 1971.

4. A. S. Platou, "Magnus Characteristics of Finned and Non-Finned Projectiles," *AIAA Journal*, Vol. 3, No. 1, January 1965.

5. H. A. Dwyer, "Methods for Computing Magnus Effects on Artillery Projectiles," BRL Contract Report No. 329, U.S. Army Ballistic Research Laboratory, Aberdeen Proving Ground, Maryland, January 1977. AD A035330.

6. W. B. Sturek, et al, "Computations of Turbulent Boundary Layer Development Over a Yawed Spinning Body of Revolution With Application to the Magnus Effect," International Symposium on Turbulent Shear Flows, The Pennsylvania State University, University Park, Pennsylvania, 18-20 April 1977. Also to be *published as a BRL Report.*

7. M. Miller, "A Technique to Measure the Pressure Distribution Acting on the Surface of a Spinning Body in a Wind Tunnel," ED-TR-76070, September 1976.

8. Kulite Semiconductor Products, Inc., "Notes on Applications of Integrated Sensor (IS) Pressure Transducer," Application Note KPS AN 11.

9. J. M. Cassanto, et al, "Use of Miniature Solid State Pressure Transducer for R/V Flight Test Application," ISA ASI 74210, 1974, pp. 33-34.

10. BRL unpublished data.
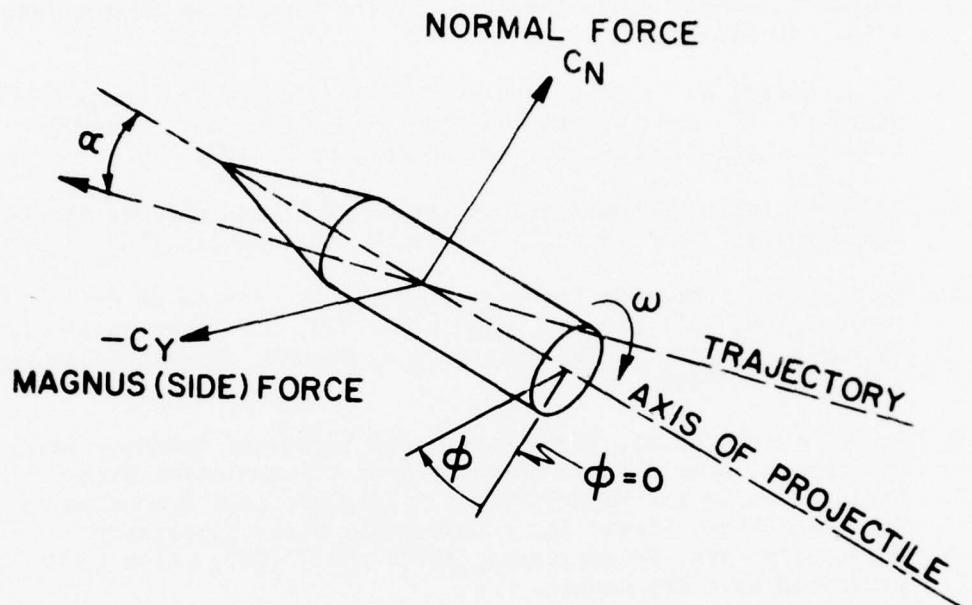
Figure 1. Magnus Force on Spinning Projectile

AIR IN

TURBINE

5.715 CM (2.25 INCH)
DIAMETER, 7.1 CAL
TANGENT-OGIVE-CYLINDER

TRANSDUCER

TRANSMITTER

POWER
&
SIGNAL
CONDITIONING

17
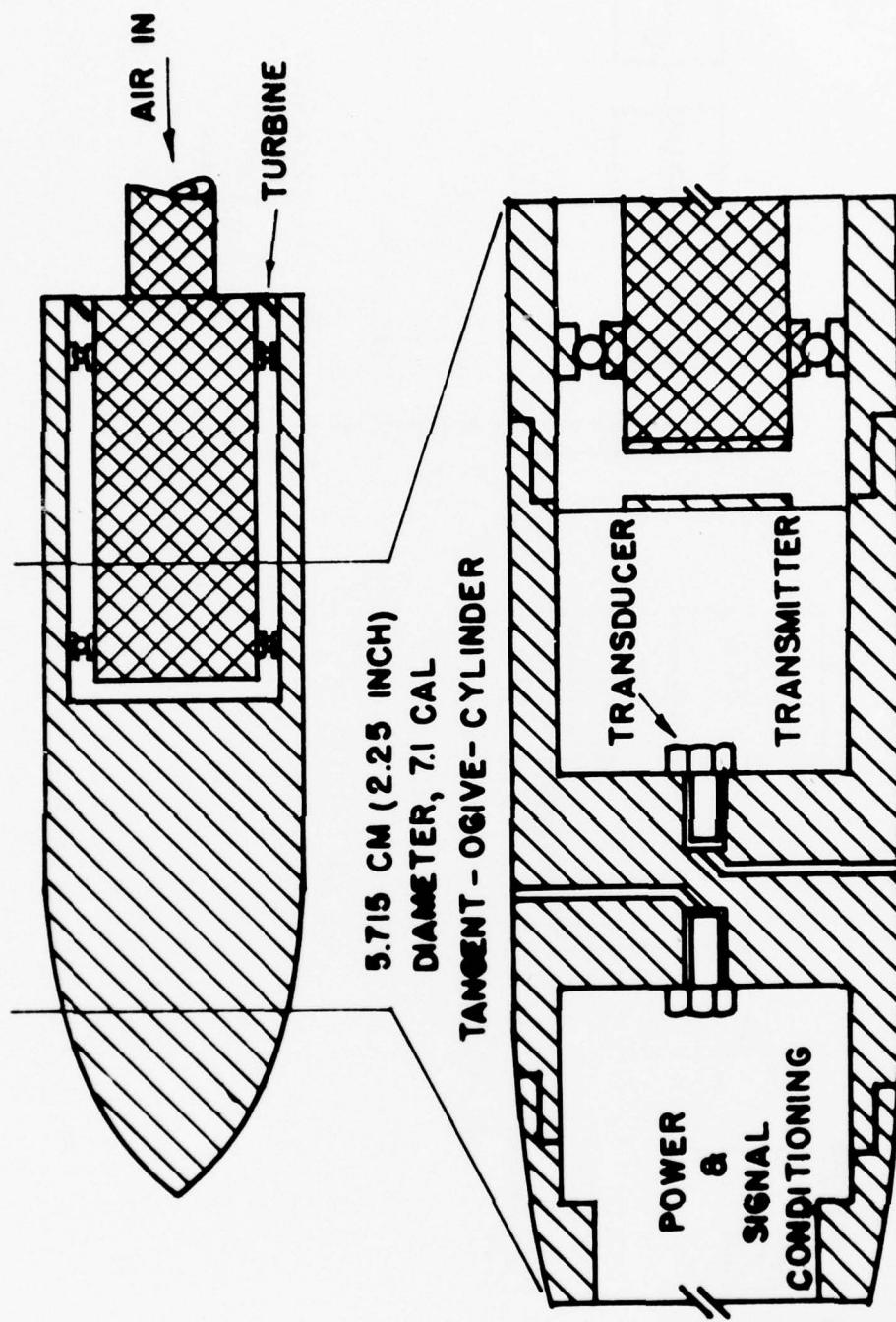
Figure 2.   Cutaway Schematic of Magnus Telemetry Model
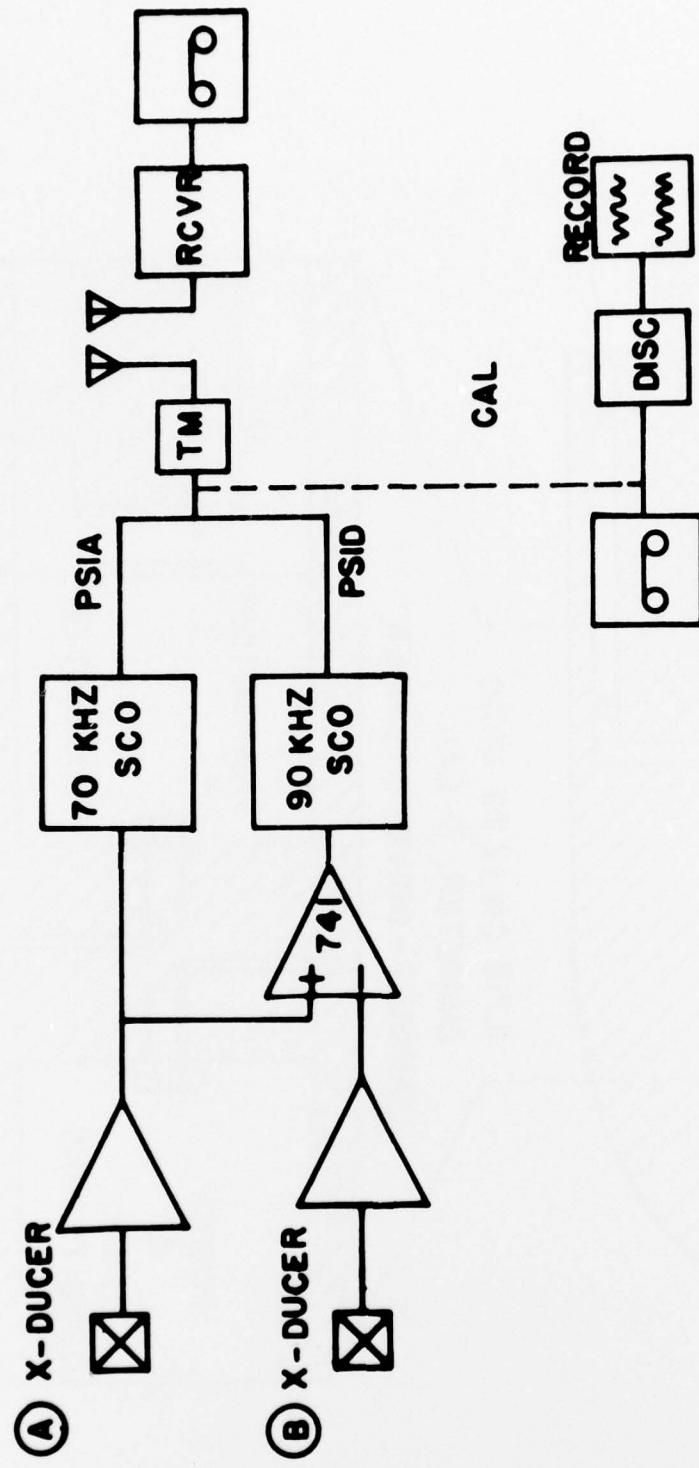
Figure 3. Block Diagram of Telemetry Transmission Link
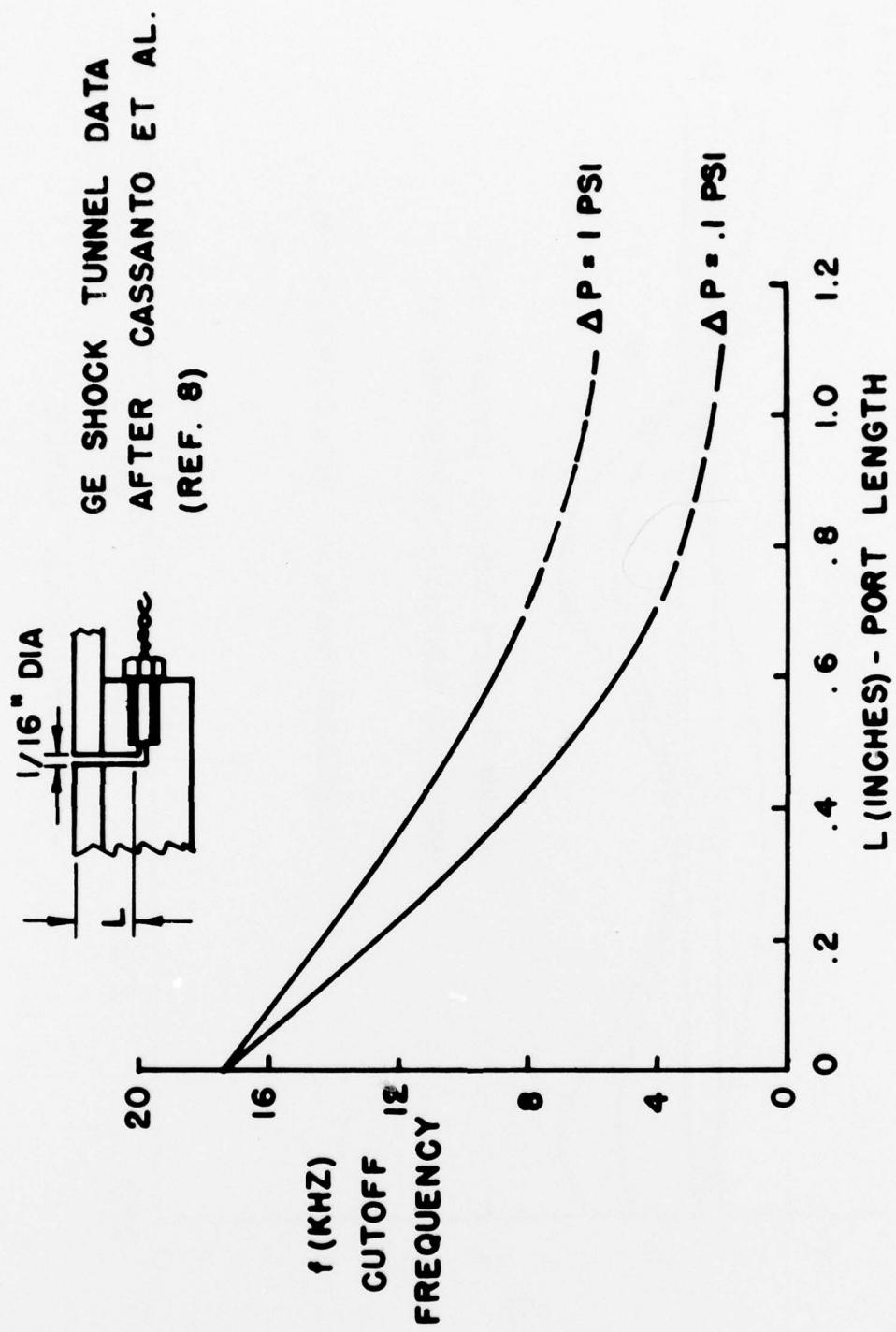
Figure 4. Frequency Response of Kulite Transducer as Measured in Shock Tube (After Cassanto, et al[8])
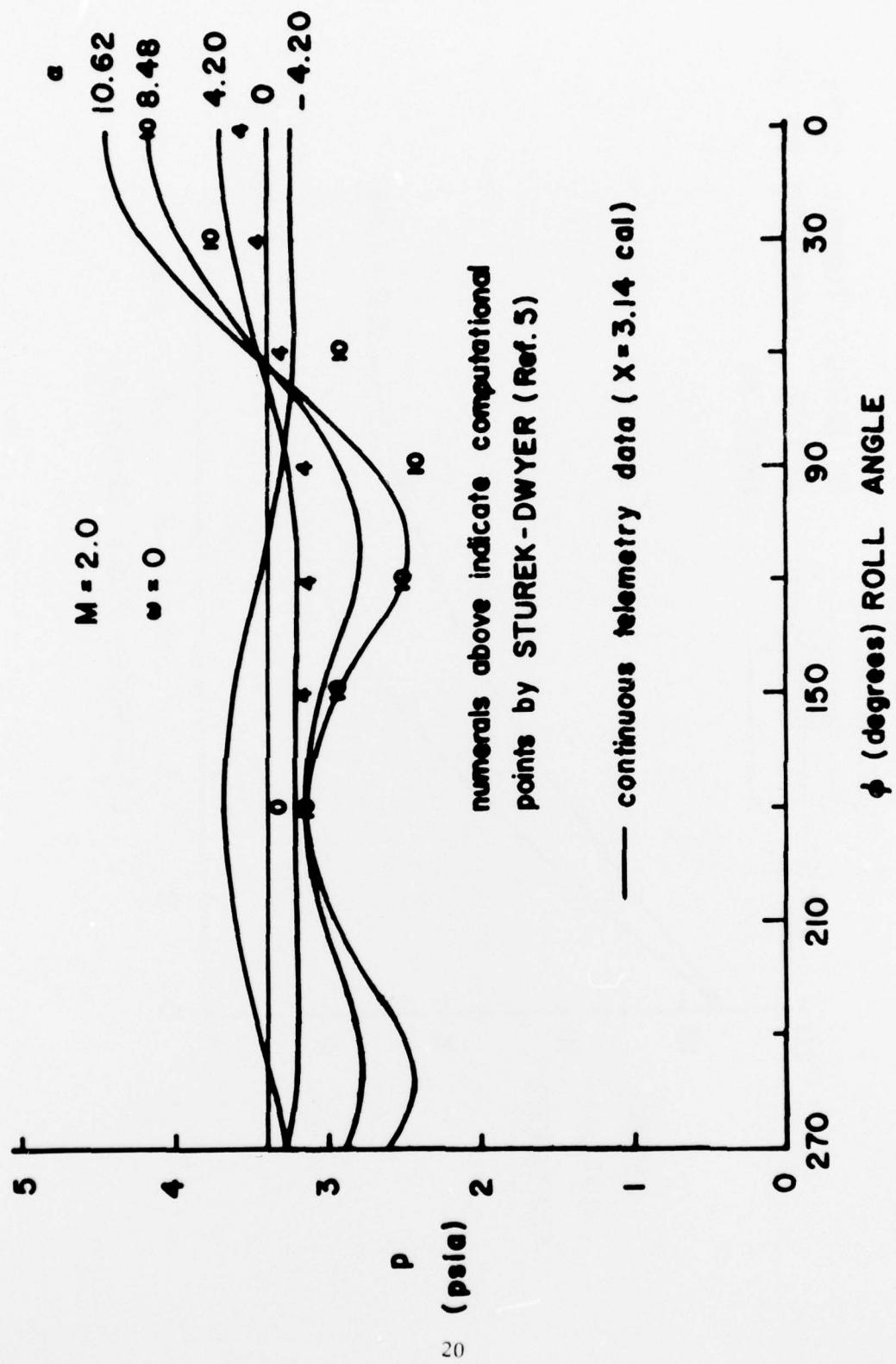
Figure 5. Surface Pressure Distribution on Tangent-Ogive-Cylinder Model at No Spin

20

M=3.0
ω=0

numerals below indicate computational
points by STUREK-DWYER (Ref.5)

—— continuous telemetry data (X=3.14 cal)

α
10.62
8.48
4.20
0
-4.20

p
(psia)

φ (degrees) ROLL ANGLE
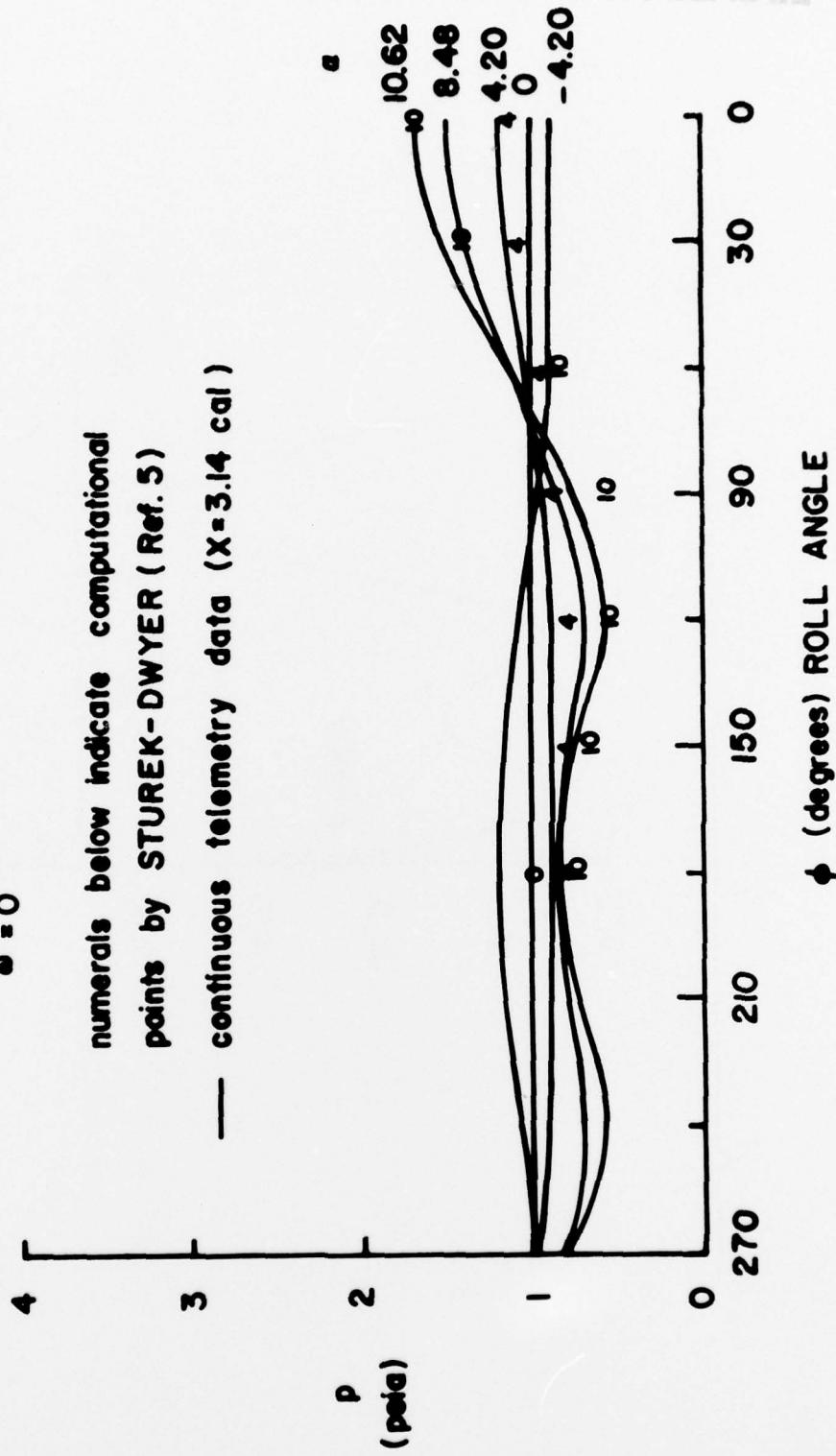
Figure 6. Surface Pressure Distribution on Tangent-Ogive-Cylinder Model at No Spin

21
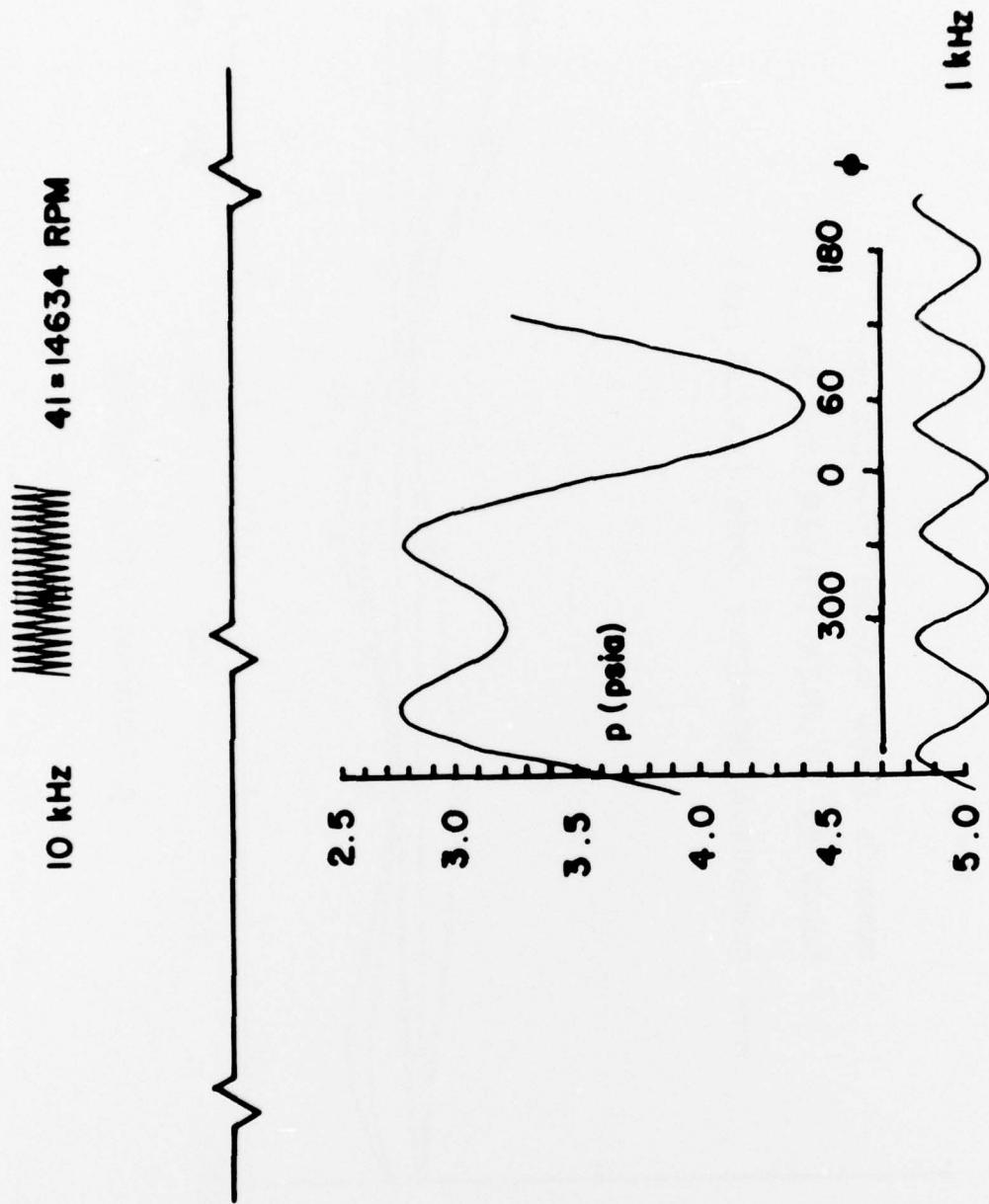
Figure 7. Raw Pressure Trace From Wind Tunnel Telemetry Model
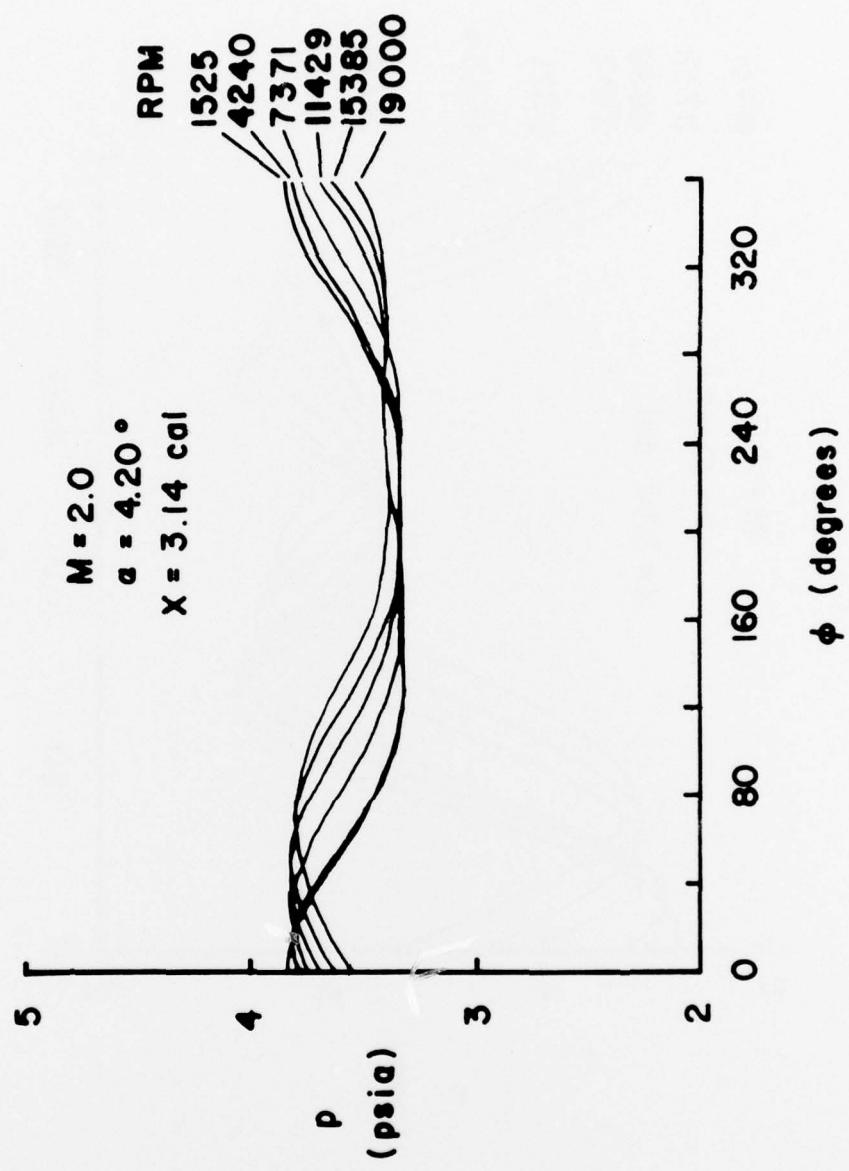
Figure 8. Surface Pressure Distribution on Tangent-Ogive-Cylinder Model With Spin
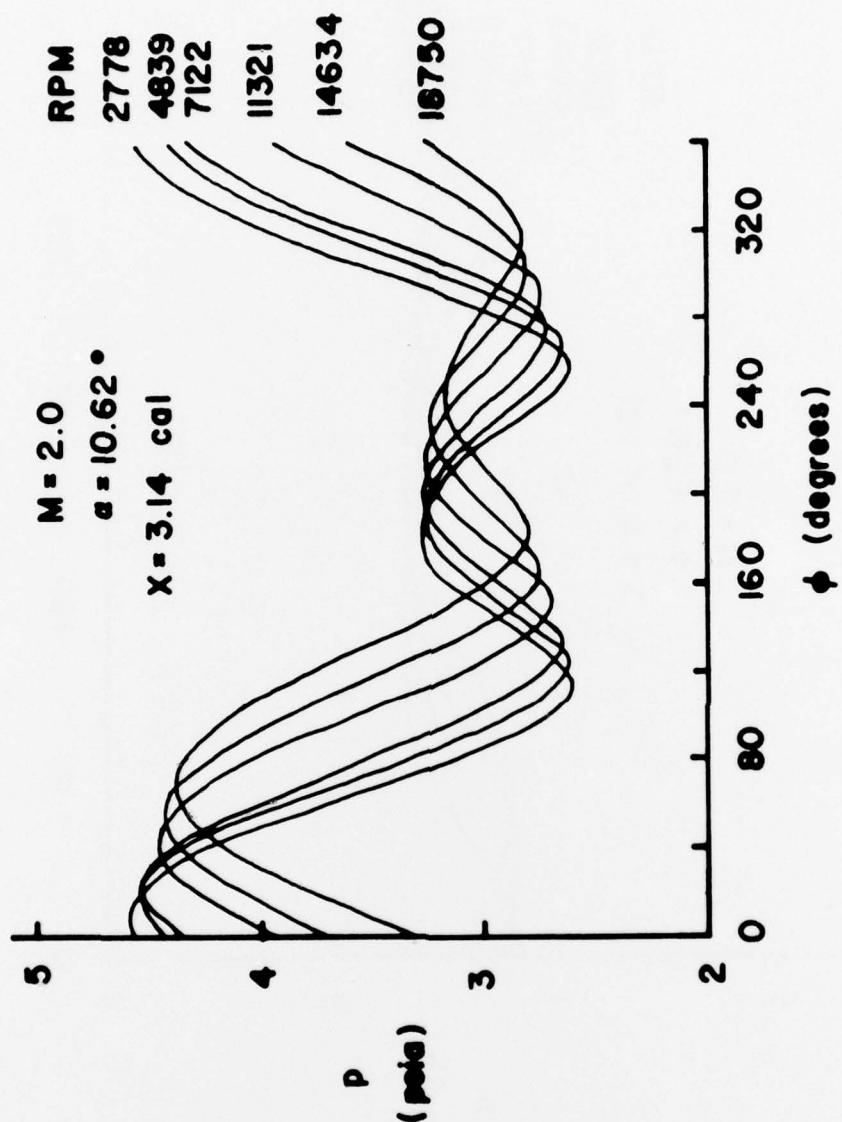
Figure 9. Surface Pressure Distribution on Tangent-Ogive-Cylinder Model With Spin

24

M = 3.5
a = 4.2°
X = 3.14 cal

RPM

3934
5742
9375
15544
20067

p
(psia)

1.2
1.0
.8
.6
.4
.2
0

0   80   160   240   320

φ (degrees)
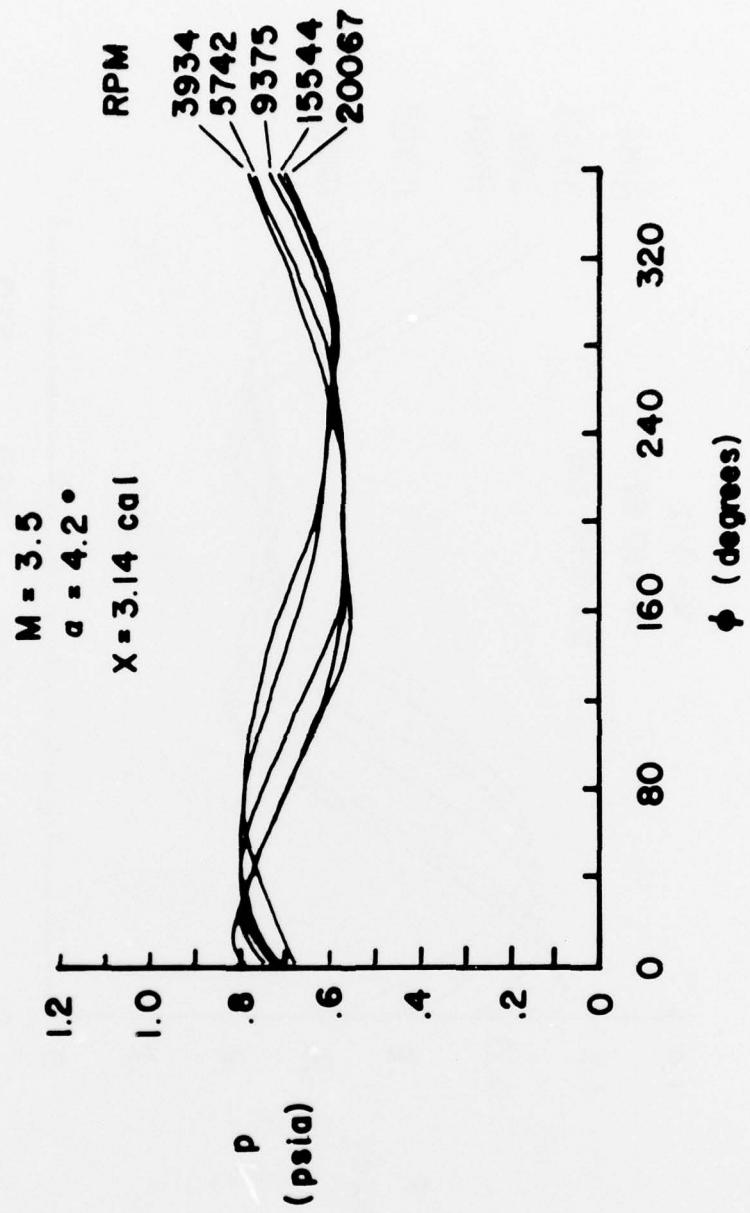
Figure 10.   Surface Pressure Distribution on Tangent-Ogive-Cylinder Model With Spin

25
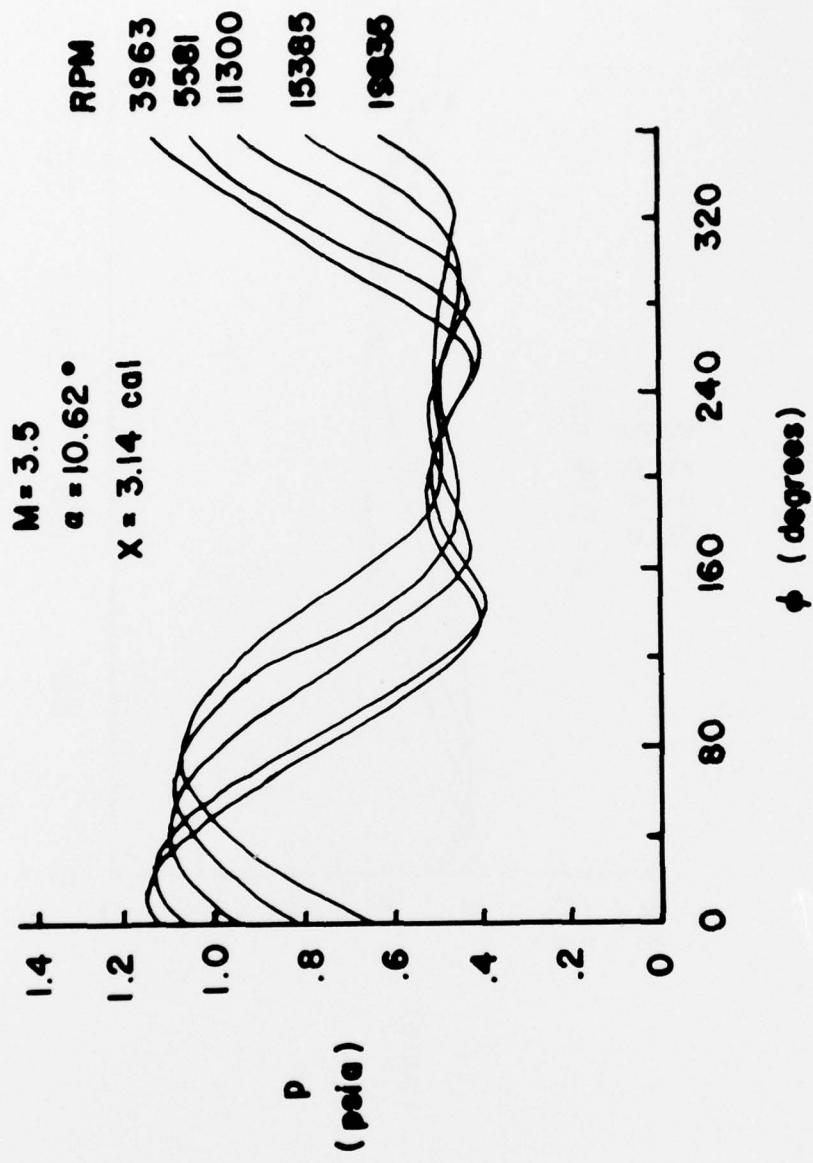
Figure 11. Surface Pressure Distribution on Tangent-Ogive-Cylinder Model With Spin
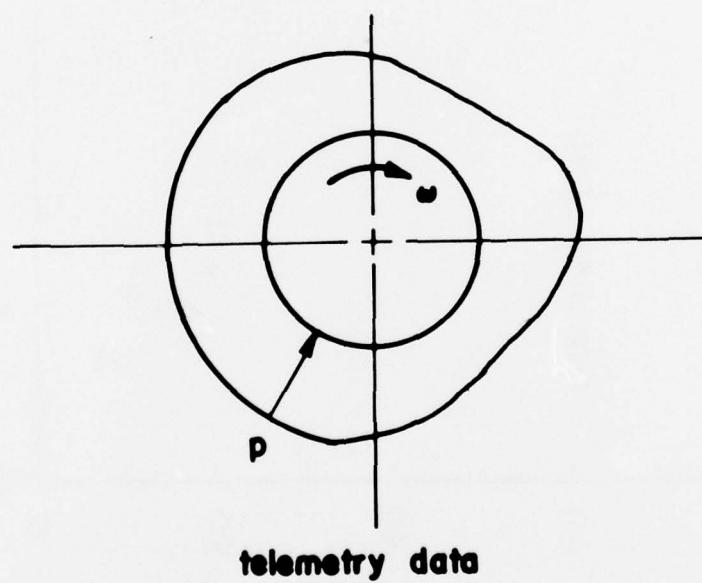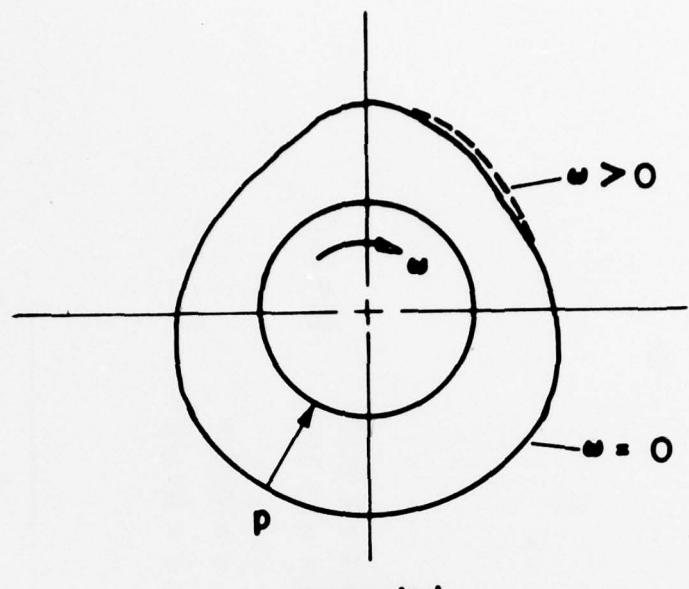
Figure 12. Peak Pressure Shift on Rotating Wind Tunnel Model

27

reference $\phi = 0$

$\bullet \; \varepsilon = 4.20°$
$\times \; \varepsilon = 10.62°$ $M = 2.0$

$\triangle \; \varepsilon = 4.20°$
$\square \; \varepsilon = 10.62°$ $M = 3.5$

RPM x 10⁻³

$\Delta \phi$ (degrees)

80 60 40 20 0

0 4 8 12 16 20

28
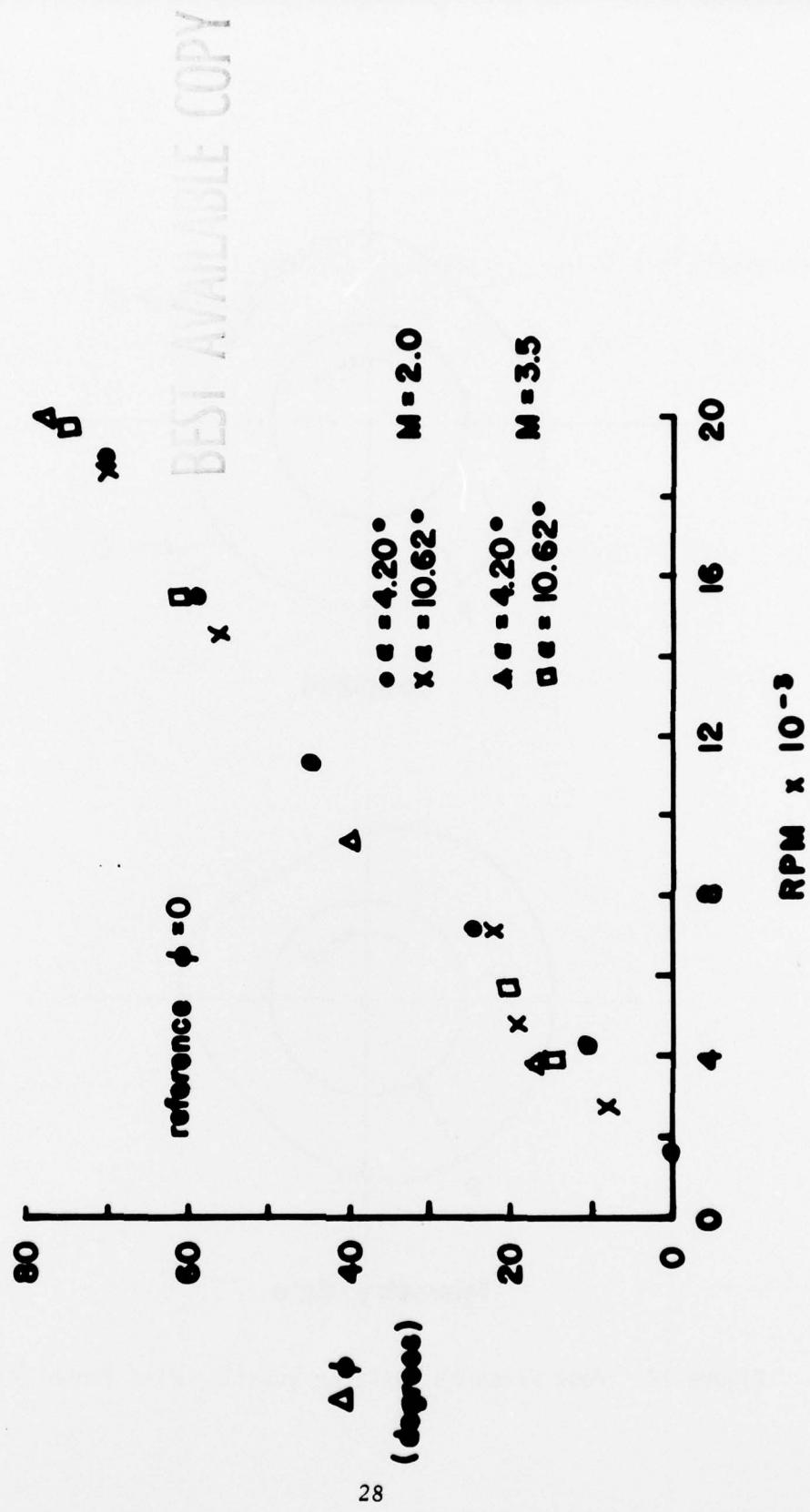
Figure 13. Graphical Display of Peak Pressure Shift in Rotating Wind Tunnel Model

DISTRIBUTION LIST

| No. of Copies	Organization	No. of Copies	Organization
12	Commander Defense Documentation Center ATTN: DDC-TCA Cameron Station Alexandria, Virginia 22314	1	Commander US Army Tank Automotive Development Command ATTN: DRDTA-RWL Warren, Michigan 48090
1	Commander US Army Materiel Development and Readiness Command ATTN: DRCDMA-ST 5001 Eisenhower Avenue Alexandria, Virginia 22333	2	Commander US Army Mobility Equipment Research and Development Command ATTN: Tech Docu Cen, Bldg 315 DRSME-RZT Fort Belvoir, Virginia 22060
1	Commander US Army Aviation Systems Command ATTN: DRSAV-E 12th and Spruce Streets St. Louis, Missouri 63166	1	Commander US Army Armament Materiel Readiness Command Rock Island, Illinois 61202
1	Director US Army Air Mobility Research and Development Laboratory Ames Research Center Moffett Field, CA 94035	4	Commander US Army Armament Research and Development Command ATTN: DRDAR-LCA-F Mr. S. Wasserman Mr. D. Mertz Mr. E. Falkowski Mr. A. Loeb Dover, New Jersey 07801
1	Commander US Army Electronics Command ATTN: DRSEL-RD Fort Monmouth, NJ 07703	2	Commander US Army Frankford Arsenal ATTN: Mr. Spencer Hirschman Mr. John Sikra Bridge and Tacony Streets Philadelphia, PA 19137
1	Commander US Army Jefferson Proving Ground ATTN: STEJP-TD-D Madison, Indiana 47250	1	Commander US Army Harry Diamond Laboratories ATTN: DRXDO-TI 2800 Powder Mill Road Adelphi, Maryland 20783
4	Commander US Army Missile Research and Development Command ATTN: DRDMI-X DRDMI-T DRDMI-TD Mr. R. Becht Mr. R. Deep Redstone Arsenal, AL 35809		

DISTRIBUTION LIST

No. of Copies	Organization
1	Commander US Army Natick Research and Development Command ATTN: DRXRE, Dr. D. Sieling Natick, Massachusetts 01762
1	Director US Army TRADOC Systems Analysis Activity ATTN: ATAA-SA White Sands Missile Range New Mexico 88002
1	Commander US Army Research Office P.O. Box 12211 Research Triangle Park North Carolina 27709
3	Commander US Naval Air Systems Command ATTN: AIR-604 Washington, D. C. 20360
2	Commander David W. Taylor US Naval Ship Research and Development Center ATTN: Dr. S. de los Santos Mr. Stanley Gottlieb Bethesda, Maryland 20084
1	Commander US Naval Surface Weapons Center ATTN: Dr. T. Clare, Code DK20 Dahlgren, Virginia 22448
2	Commander US Naval Surface Weapons Center ATTN: Code 312, Mr. S. Hastings Code 312, Mr. F. Regan Silver Spring, Maryland 20910

No. of Copies	Organization
1	Commander US Naval Weapons Center ATTN: Code 5115 Dr. A. Charters China Lake, California 93555
1	AFATL (DLDL) Eglin AFB Florida 32542
1	Director Jet Propulsion Laboratory ATTN: Mr. B. Dayman 4800 Oak Grove Drive Pasadena, California 91103
1	Calspan Corporation ATTN: Mr. J. Andes, Head Transonic Tunnel Dept. P.O. Box 235 Buffalo, New York 14221
1	Honeywell, Inc. ATTN: Mr. George Stilley 600 Second Street, N. Hopkins, Minnesota 55343
1	Sandia Laboratories ATTN: Division No. 9322 Mr. Warren Curry P.O. Box 5800 Albuquerque, New Mexico 87115
2	Massachusetts Institute of Technology ATTN: Prof. E. Covert Prof. C. Haldeman 77 Masschusetts Avenue Cambridge, Massachusetts 02139

DISTRIBUTION LIST

No. of Copies	Organization	No. of Copies	Organization

1	MIT/Lincoln Laboratories
	ATTN: Dr. Milan Vlajinac
	        Mail Stop D-382
	P.O. Box 73
	Lexington, Massachusetts
	02173
		1	University of Virginia
			Department of Aerospace
			    Engineering and Engineering
			    Physics
			ATTN: Prof. I. Jacobson
			Charlottesville, Virginia
			22904

1	Rutgers University
	Mechanical, Industrial, and
	    Aerospace Engineering
	    Department
	ATTN: Dr. Robert H. Page
	New Brunswick, New Jersey
	08903		

Aberdeen Proving Ground

Marine Corps Ln Ofc
Director, USAMSAA